Loss of complexity characterizes the heart rate response to experimental hemorrhagic shock in swine*

Andriy I. Batchinsky, MD; William H. Cooke, PhD; Tom Kuusela, PhD; Leopoldo C. Cancio, MD

Objective: **To improve our ability to identify physiologic deterioration caused by critical illness, we applied nonlinear and frequency-domain analytical methods to R-to-R interval (RRI) and systolic arterial pressure (SAP) time series during hemorrhagic shock.**

Design: **Prospective, randomized, controlled trial.**

Setting: **Animal laboratory of a government research institute.**

Subjects: **Twenty swine (weight 36.4 ± 0.11 kg).**

Interventions: **Fixed-volume hemorrhage followed by resuscitation; off-line analysis of RRI and SAP data.**

Measurements and Main Results: **Anesthetized swine (shock group, n = 12) underwent withdrawal of 30 mL/kg blood in 10 mL/kg decrements. A control group (n = 8) received maintenance fluids only. Electrocardiogram and arterial pressure waveforms were acquired at 500 Hz. Eight hundred-beat data sets were analyzed at six time points: at baseline, after each blood withdrawal, after lactated Ringer's resuscitation, and after infusion of shed blood. Nonlinear methods were used to estimate the complexity (approximate entropy, sample entropy, Lempel-Ziv entropy, normalized entropy of symbol dynamics), RRI bits per word, and fractal dimension by curve lengths and by dispersion analysis of the RRI and SAP time series. Fast Fourier transformation was used to measure the high-frequency and low-frequency powers of RRI and SAP. Baroreflex sensitivity was assessed in the time domain with the sequence method. Hemorrhagic shock caused decreases in RRI complexity as quantified by approximate entropy, sample entropy, and symbol dynamics; these changes were reversed by resuscitation. Similar but statistically insignificant changes in fractal dimension by curve lengths were seen. RRI high-frequency power decreased with hemorrhagic shock—indicating withdrawal of vagal cardiac input—and was restored by resuscitation. Similar changes in baroreflex sensitivity were seen. Hemorrhagic shock did not affect SAP complexity.**

Conclusions: **Hemorrhagic shock caused a reversible decrease in RRI complexity; these changes may be mediated by changes in vagal cardiac control. Assessment of RRI complexity may permit identification of casualties with hemorrhagic shock. (Crit Care Med 2007; 35:519–525)**

KEY WORDS: shock; hemorrhage; electrocardiography; heart rate variability; fractals; nonlinear dynamics; spectrum analysis

Noninvasive monitoring may revolutionize the care of the critically ill if data analysis techniques can be validated that identify physiologic deterioration before changes in conventional vital signs. In pursuit of this goal, frequency-domain measures of heart rate variability (HRV) have been proposed, enabling noninvasive quantification of the autonomic modulation of the heart rate (1, 2). HRV metrics have been associated with changes in volume status (3, 4) and in the depth of anesthesia (5), "inappropriate" vagal predominance has been associated with adverse outcomes in trauma patients (6), and loss of HRV has been predictive of death in critically ill humans (7, 8). The frequency-domain approach has also been criticized (9). The results obtained are affected by the methodology used (10); data analysis assumes signal stationarity, a condition difficult to achieve; and the approach has not been designed to unveil the inherent dynamic properties of complex cardiovascular regulatory systems (11). As pointed out by Goldberger and West (12) and Buchman (13), physiologic systems exhibit marked signal variability, constantly change over time, and operate in nonlinear states.

In linear systems, the magnitude of response is proportionate to the strength of the stimulus. In a nonlinear system, by contrast, proportionality does not hold; the components of this system are coupled and interact, causing abrupt changes (14). Such systems are better described by nonlinear statistics that determine the degree of regularity or irregularity in the system (15).

Because frequency-domain methods assume system linearity, nonlinear statistical methods have increasingly been applied to HRV analysis (5, 7, 11, 16–18). Use of these methods is predicated on the concept that *complexity* is a fundamental characteristic of normal physiologic data such as the R-to-R interval (RRI) time series (16), whereas loss thereof, or "decomplexification," is a feature of disease (12) and of impaired adaptation to physiologic stress (19). For example, loss of RRI complexity as manifested by decreases in approximate entropy (ApEn), and alterations in fractal scaling properties, have both been identified with aging

***See also p. 656.**

From the U.S. Army Institute of Surgical Research, Fort Sam Houston, TX (AIB, LCC); Department of Health and Kinesiology, University of Texas at San Antonio, San Antonio, TX (WHC); and Department of Physics, University of Turku, Turku, Finland (TK).

Supported, in part, by grant DAMD 17-02-1-0714 from Technologies for Metabolic Monitoring 2002 and by the Combat Casualty Care Research Program, U.S. Army Medical Research and Materiel Command, Fort Detrick, MD.

Presented at the Society of Critical Care Medicine Annual Meeting, Phoenix, AZ, January 16, 2005.

The authors have not disclosed any potential conflicts of interest.

The opinions or assertions contained herein are the private views of the authors, and are not to be construed as official or as reflecting the views of the Department of the Army or the Department of Defense.

DOI: 10.1097/01.CCM.0000254065.44990.77

Report Documentation Page

Form Approved
OMB No. 0704-0188

1. REPORT DATE	2. REPORT TYPE	3. DATES COVERED
01 FEB 2007	**N/A**	**-**

4. TITLE AND SUBTITLE	5a. CONTRACT NUMBER
Loss of complexity characterizes the heart rate response to experimental hemorrhagic shock in swine	5b. GRANT NUMBER
	5c. PROGRAM ELEMENT NUMBER
6. AUTHOR(S)	5d. PROJECT NUMBER
Batchinsky A. I., Cooke W. H., Kuusela T., Cancio L. C.,	5e. TASK NUMBER
	5f. WORK UNIT NUMBER
7. PERFORMING ORGANIZATION NAME(S) AND ADDRESS(ES)	8. PERFORMING ORGANIZATION REPORT NUMBER
United States Army Institute of Surgical Research, JBSA Fort Sam Houston, TX 78234	
9. SPONSORING/MONITORING AGENCY NAME(S) AND ADDRESS(ES)	10. SPONSOR/MONITOR'S ACRONYM(S)
	11. SPONSOR/MONITOR'S REPORT NUMBER(S)

12. DISTRIBUTION/AVAILABILITY STATEMENT
Approved for public release, distribution unlimited

13. SUPPLEMENTARY NOTES

14. ABSTRACT

15. SUBJECT TERMS

16. SECURITY CLASSIFICATION OF:			17. LIMITATION OF ABSTRACT	18. NUMBER OF PAGES	19a. NAME OF RESPONSIBLE PERSON
a. REPORT	b. ABSTRACT	c. THIS PAGE			
unclassified	**unclassified**	**unclassified**	**UU**	**7**	

(19–21). Decrease of RRI fractal scaling was documented in heart failure and in Chagas' disease (22); was predictive of mortality after myocardial infarction (18, 23) and stroke (24), as well as of ischemia after coronary artery bypass grafting (25); and distinguished subjects with coronary artery disease from healthy controls (17).

Reports on the assessment of complexity during hypovolemia or hemorrhagic shock (HS) are scarce. Decreased ApEn following prolonged bed rest was associated with reduced tolerance to central hypovolemia induced by lower body negative pressure (LBNP) (26). Decrease in the complexity of the HR but not of the blood pressure has been documented in healthy humans during orthostatic stress secondary to LBNP (3). Hemodialysis-induced hypotension decreased ApEn in patients with and without diabetes mellitus (27). In dogs, Palazzolo et al. (28) identified a decrease in RRI ApEn and symbol dynamics entropy (SymDyn) secondary to hypotension.

The objective of this study was to determine whether loss of RRI and systolic arterial pressure (SAP) complexity is a characteristic of HS. We hypothesized that hemorrhage causes loss of complexity in these signals and that resuscitation restores it. Several different, but potentially complementary, nonlinear methods were used.

MATERIALS AND METHODS

This study was approved by the U.S. Army Institute of Surgical Research Animal Care and Use Committee and was carried out in accordance with the guidelines set forth by the Animal Welfare Act, other federal statutes and regulations, and the 1996 *Guide for the Care and Use of Laboratory Animals* of the National Research Council.

Animal Preparation. Twenty female Yorkshire pigs (hemorrhage group n = 12, control group n = 8) weighing 36.4 ± 0.11 kg SEM were fasted for 24 hrs, anesthetized with a combination of isoflurane (0.62 ± 0.04%) and intravenous ketamine (332.1 ± 10.4 SEM μg/kg/hr) (Ketamine Hydrochloride, St. Joseph, MO), and volume-control ventilated with room air at a tidal volume of 10 mL/kg and respiratory rate of 12 per minute. Respiratory rate was adjusted at baseline to maintain normocapnia ($Paco_2$ = 35–45 mm Hg) and was kept constant throughout the study to standardize the effect of respiration on HRV (29, 30). Bilateral surgical catheterizations of the carotid arteries and external jugular veins and a midline laparotomy and splenectomy (to preclude autoresuscitation during hemorrhage) were performed. Each animal received a bolus of lactated Ringers' solution (LR) equivalent to 1.5 times the spleen weight. Arterial blood pressure (ABP) was measured via the carotid line and was transduced (Transpac IV, Abbott, North Chicago, IL) at heart level. The heart rate was obtained from the electrocardiogram.

Experimental Protocol. After 1 hr of baseline stabilization, the experimental protocol was started (Table 1). In the hemorrhage group, blood was manually withdrawn via a syringe from the left carotid artery catheter during each of three 10-min bleeding periods at a constant rate of 1 mL/kg/min, for a total bleed of 30 mL/kg. This approximated a 45% hemorrhage. The blood was collected into commercial collection bags containing CPD anticoagulant (Terumo, Tokyo, Japan). Each bleed period was followed by a 15-min stabilization period. After the third bleed, the pigs were resuscitated with two times the shed blood volume of LR, followed by reinfusion of shed blood. LR resuscitation and blood reinfusion were performed with the 245 Ranger (Blood/Fluid) Warming System (Augustine Medical, Eden Prairie, MN). The animals were observed for 30 mins thereafter and then were killed by an overdose of sodium pentobarbital (Fatal-Plus, Dearborn, MI). Animals in the control group received a maintenance LR infusion at a 2 mL/kg/hr rate only.

Waveform Analysis. Electrocardiogram and ABP waveforms were continuously monitored throughout the experiment and recorded at 500 Hz for off-line analysis during discrete 15-min observation periods. This allowed us to do the analysis on relatively stable data sets collected during periods between interventions (i.e., episodes of blood withdrawal, resuscitation, or blood reinfusion). Six time points (baseline, after bleed 1, after bleed 2, after bleed 3, after LR resuscitation, and after blood reinfusion, Table 1) were analyzed for every subject. Next, 800-beat data sets from within each 15-min waveform recording were imported into WinCPRS software (Absolute Aliens Oy, Turku, Finland). Eight hundred beats were selected because nonlinear statistics are sensitive to changes in the number of data points (especially ApEn). Automatic identification of R-waves was carried out by means of an isoelectric line-shift algorithm. We manually verified correct identification of R-waves by the software in every data set. Whenever possible, ectopic beats (EBs) were avoided by selecting an 800-beat section free from ectopy. When present, EBs were replaced by a linear interpolation function of the software. Of the 20 animals included in this study, EBs were identified at a few time points in ten of them. However, in most cases (eight of ten), only one EB was identified within the 800-beat segment analyzed, accounting for a 0.13% interpolation rate per 800 beats. In the remaining two of ten animals with EBs, three, 12, and 15 EBs were identified within three separate 800-beat segments, accounting for 0.38%, 1.5%, and 1.8% interpolation rates, respectively.

The software generated the instantaneous RRI and SAP time series. Before spectral calculations, signals were windowed with Hanning function and resampled with a five sample per second rate. The resampled signals were zero-padded to the next power of 2 before the FFT routine was used to calculate the power spectra. Next, the total power spectral density (TP, frequency range: 0.003–0.4 Hz), the low-frequency power (LFP; frequency range, 0.04–0.15 Hz) and high-frequency power (HFP; frequency range, 0.15–0.4 Hz) components of the RRI and SAP spectra were calculated for each data set with baseline normalization. The LFP/HFP ratio of the RRI was taken as an index of sympathovagal balance (1, 2). The integrated baroreflex sensitivity (BRS), ApEn, sample entropy (SampEn), Lempel-Ziv entropy, SymDyn, RRI bits per word, fractal dimension by curve lengths (FDCL), and fractal dimension by dispersion analysis were calculated for the RRI and SAP time series in the same 800-point data sets using the WinCPRS software, as described by Kuusela et al. (11) (Appendix). Before entropy calculations, linear trends were removed.

Statistical Analysis. Nonnormal data were $\log_{10}$-normalized if possible. Independent samples *t*-tests or Mann-Whitney U tests

Table 1. Experimental protocol

Time Point	Duration, Mins	Event
Baseline	30	EKG and ABP waveform recording
Hemorrhage 1	10	Constant rate 1 ml·kg·min bleed
Recovery 1	15	Observation/EKG and ABP waveform recording
Hemorrhage 2	10	Constant rate 1 ml·kg·min bleed
Recovery 2	15	Observation/EKG and ABP waveform recording
Hemorrhage 3	10	Constant rate 1 ml·kg·min bleed
Recovery 3	15	Observation/EKG and ABP waveform recording
LR infusion	25	1.5 times the shed volume of LR infused
Observation	30	Observation/EKG and ABP waveform recording
Blood reinfusion	25	Reinfusion of shed blood
Observation	30	Observation/EKG and ABP waveform recording
Total study time	215	

EKG, electrocardiogram; ABP, arterial blood pressure; LR, lactated Ringers' solution.

Table 2. Study results

Group	Baseline	10 mL	20 mL	30 mL	Post-LR	Post-Tx	p*	p**	p***	p†
RRI mean										
C	618	629	634	646	649	640				
B	676	600	475*	388**	493***	570	.002	<.001	.003	
SAP mean										
C	94	97	98	98	89	88				
B	100	77*	70**	53**	80	105***	.002	<.001	.012	
RRI ApEn										
C	1.26	1.20	1.12	1.04	1.14	1.08				
B	1.21	1.03	1.00	0.76*	0.99	1.09	.017			
RRI SampEn										
C	1.35	1.28	1.22	1.10	1.20	1.12				
B	1.29	1.04	0.99	0.71*	0.95**	1.11	.010	.017		
RRI SymDyn										
C	0.73	0.72	0.66	0.67	0.67	0.67				
B	0.68	0.58*	0.61	0.50**	0.64	0.70	.034	.013		
RRI FDCL										
C	1.88	1.86	1.81	1.77	1.79	1.76				
B	1.82	1.74	1.74	1.62	1.76	1.79	NS			
RRI BPW										
C	4.40	4.32	3.99	4.02	4.04	4.00				
B	4.10	3.49*	3.69	3.00**	3.83	4.20	.034	.013		
RRI FDDA										
C	1.15	1.21	1.20	1.16	1.12	1.18				
B	1.07	1.06*	1.06**	1.05***	1.05†	1.08	.012	.025	.008	.021
RRI HFP										
C	8.36	9.95	9.58	11.55	9.69	7.94				
B	3.76	2.27	1.02*	0.23**	2.21***	3.65	.004	<.001	.015	
SAP HFP										
C	4.50	5.11	5.03	4.38	5.47	7.85				
B	5.69	9.90	23.90*	27.25**	18.49***	2.84†	.001	.019	.012	.004
BRS										
C	1.33	1.36	1.39	1.35	1.26	0.83				
B	0.94	0.61*	0.24**	0.15**	0.36***	1.02	.029	<.001	<.001	.002

Baseline, baseline data collection; 10 mL, 20 mL, 30 mL, data collection after 10 mL, 20 mL, or 30 mL, respectively, of blood removed; Post-LR, after resuscitation with Ringers' lactate; Post-TX, after blood reinfusion; p*, p**, p***, and p†, levels of significance for values in the bleed vs. control groups at each time point by independent samples or Mann Whitney U tests; RRI, R-to-R interval; C, control group; B, bleed group; SAP, systolic arterial pressure; ApEn, approximate entropy; SampEn, sample entropy; SymDyn, symbol dynamics entropy; FDCL, fractal dimension by curve lengths; BPW, bit per word; FDDA, fractal dimension by dispersion analysis; HFP, high-frequency power; BRS, baroreflex sensitivity.

Data are mean ± SEM.

were performed at each time point, control vs. bleed groups. Significance was accepted at $p < .05$.

RESULTS

Study results are summarized in Table 2. In response to hemorrhage, the RRI decreased linearly, differed from controls after the second bleed, and was restored to control values by reinfusion of shed blood (Table 2 and Fig. 1). SAP (Fig. 2) differed from controls after the first bleed and was restored by LR resuscitation.

The ApEn, SampEn, and SymDyn (Fig. 3*A* and 3*B*; Table 2) of the RRI all showed similar graphic appearance, decreased with hemorrhage, and were restored by resuscitation. An analogous trend was observed in FDCL (Fig. 3*C*), although these differences were not significant. RRI bits per word differed after the first and third bleeds (Table 2). The values of fractal dimension by dispersion analysis were systematically lower in the hemorrhaged animals and differed from controls after the first bleed (Table 2). RRI Lempel-Ziv entropy did not change (data not shown). Changes in SAP ApEn, SampEn, SymDyn, Lempel-Ziv entropy, FDCL, fractal dimension by dispersion analysis, and bits per word were not significant and are not shown.

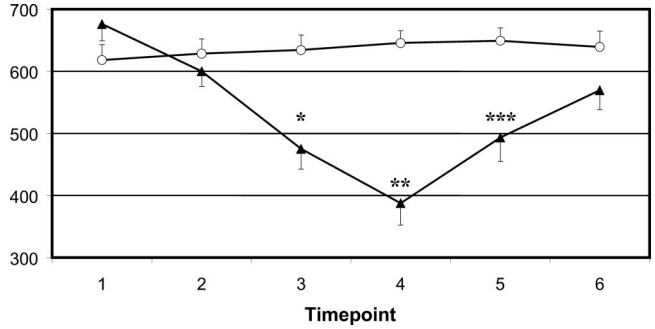

Figure 1. Changes in R-to-R interval over time. *Triangles*, hemorrhaged animals; *circles*, controls. For statistical significance, see Table 2. t-tests: *$p = .002$; **$p < .001$; ***$p = .003$.

Spectral analysis revealed a significant decrease in RRI HFP (Fig. 4*A*), which was reversed by resuscitation. SAP HFP increased with hemorrhage, differed between groups after bleed 2, and remained significantly increased until

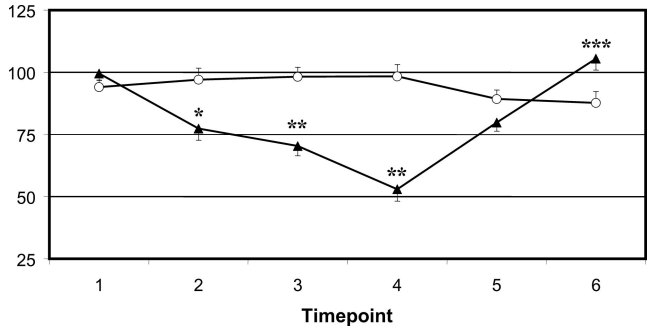

Figure 2. Changes in systolic arterial pressure over time. *Triangles*, hemorrhaged animals; *circles*, controls. *t*-tests: *$p = .002$; **$p < .001$; ***$p = .012$.

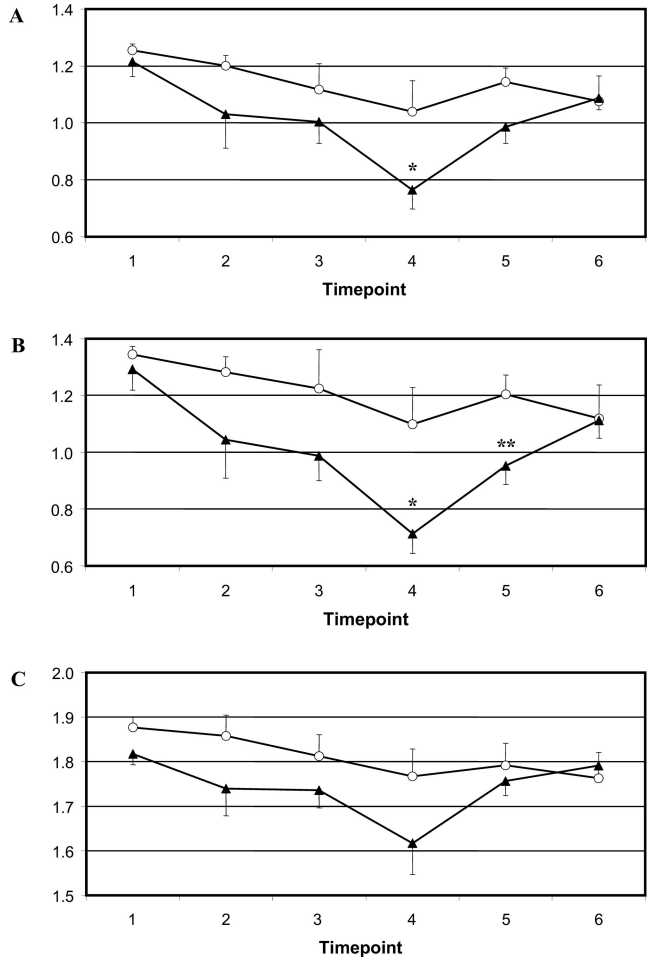

Figure 3. *A*, changes in R-to-R interval approximate entropy over time. *Triangles*, hemorrhaged animals; *circles*, controls. Mann-Whitney U tests: *$p = .017$. *B*, changes in RRI sample entropy over time. *Triangles*, hemorrhaged animals; *circles*, controls. Mann-Whitney U tests: *$p = .010$; **$p = .017$. *C*, changes in RRI fractal dimention by curve lengths over time. *Triangles*, hemorrhaged animals; *circles*, controls. Not significant.

blood reinfusion (Fig. 4*B*). SAP TP increased in concert with the SAP HFP (data not shown). Changes in RRI LFP/HFP ratio, RRI LFP, RRI TP, and SAP LFP were not significant (data not shown). BRS decreased with hemorrhage and was restored by resuscitation (Fig. 4*C*).

DISCUSSION

The principal finding of this study is that RRI complexity, as assessed by several complementary measures, decreases after controlled 30 mL/kg hemorrhage in anesthetized and mechanically ventilated swine. Loss of complexity occurred in association with decreases in vagal cardiac oscillations (as quantified by the RRI HFP) and in cardiovagal baroreflex sensitivity. All of these values were restored by resuscitation.

One of the most frequently used complexity measures was introduced by Pincus (31) and involves quantification of the degree of *entropy* in the system as an approximate measure of complexity. Hornero et al. (32) stated that ApEn is a robust approximate complexity metric of a signal that combines information on HRV and the number of signal harmonics and correlates with the signal-noise bandwidth. Another common complexity measure, SampEn, was introduced by Richman and Moorman (33) and is based on ApEn with a computational refinement (Appendix). In our study, ApEn and SampEn both decreased with HS and were restored with resuscitation. Previously, Palazzolo et al. (28) documented a decrease in ApEn secondary to hypotension in dogs. Using selective and combined blockade of the autonomic system branches, the authors showed that under various physiologic conditions (rest, standing, hypotension), entropy reflects the parasympathetic modulation of the heart rate (28). In a study in healthy humans, Penttila et al. (34) found that vagal blockade decreased both the ApEn and the fractal scaling of the RRI. Similarly, in our study the decrease in various complexity measures was associated with evidence of vagal withdrawal.

The fractal dimension of the RRI time series is another complexity measure explored in this study. As measured by FDCL (Appendix), the RRI fractal dimension changed nonsignificantly, although in concert with the other complexity metrics. These results are similar to data presented by Kuusela et al. (11), in which FDCL decreased along with ApEn secondary to terbutaline administration in humans. Also, West et al. (35) found a decline in RRI fractal dimension in subjects during central hypovolemia induced by LBNP.

The SymDyn and bits per word methods used here for quantifying complexity are computationally quite different from the ApEn and fractal methods (Appendix). Nevertheless, changes in these variables paralleled those of the entropy and fractal dimension. Palazzolo et al. (28) showed decreased SymDyn during rest, standing, and systemic hypotension in dogs as a function of vagal withdrawal. SymDyn was decreased by terbutaline infusion in

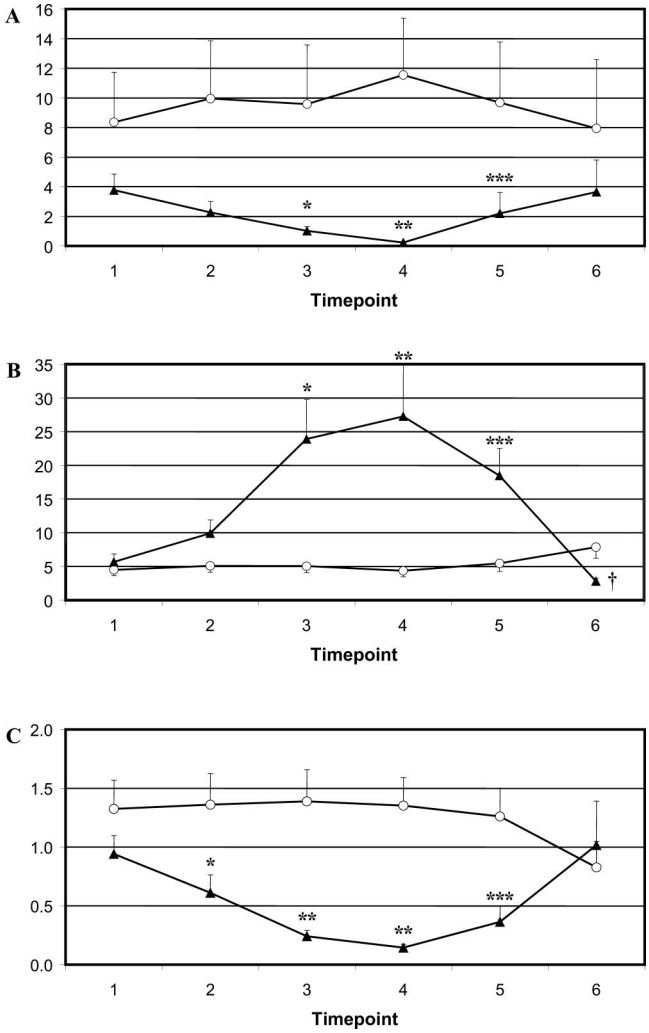

Figure 4. *A*, changes in R-to-R interval high-frequency power over time. *Triangles*, hemorrhaged animals; *circles*, controls. *t*-tests (log-transformed data): $*p = .004$; $**p < .001$; $***p = .015$. *B*, changes in systolic arterial pressure (*SAP*) high-frequency power over time. *Triangles*, hemorrhaged animals; *circles*, controls. *t*-tests (log-transformed data): $*p = .001$; $**p = .019$; $***p = .012$; $\dagger p = .004$. *C*, changes in R-to-R interval integrated baroreflex sensitivity over time. *Triangles*, hemorrhaged animals; *circles*, controls. Mann-Whitney U tests: $*p = .029$; $**p < .001$; $***p = .002$.

humans (11) most likely due to decreases in parasympathetic cardiovascular regulation (36).

In contrast to the RRI metrics, measures of SAP complexity did not change in our study—yielding results similar to those of Butler et al. (3), who identified a decrease in RRI but not in ABP complexity in healthy humans during LBNP assessed by detrended fluctuations. As suggested by Kuusela et al. (11), the RRI and SAP may have different underlying dynamic structures, with the former being more complex and the latter more regular and much simpler then the regulation of the heart rate.

Frequency-domain HRV analyses have been extensively applied to critically ill humans and have yielded important findings. Goldstein et al. (7) found that illness severity scores correlated inversely with LFP and HFP of the RRI in critically ill and injured pediatric patients. The same group also differentiated brain-dead and non-brain-dead pediatric patients with severe brain injury using HRV analysis (37). Winchell and Hoyt (8) found that low sympathetic activity relative to vagal activity predicted death in ICU patients, whereas sympathetic predominance was associated with survival. Cooke et al. (6) applied HRV analysis to trauma patients during prehospital transport. Death was predicted by parasympathetic predominance.

In contrast with the previously mentioned studies in which relative vagal predominance predicted mortality, the decrease in RRI HFP observed in our nonlethal study suggests that progressive, compensatory cardiac parasympathetic withdrawal occurred in response to HS. Previously, Kawase et al. (38) found that both LFP and HFP decreased with progressive blood loss in anesthetized, mechanically ventilated dogs. Similarly, Butler et al. (3) documented cardiac parasympathetic withdrawal and sympathetic stimulation secondary to LBNP in humans. Triedman et al. (39) also established a significant decrease in vagal modulation of the heart in humans during blood donations.

Lack of significance in the changes in LFP/HFP ratio in our study may reflect the effects of anesthesia on HRV, which alters sympathetic compensation for HS (5, 40, 41). In our study, integrated baroreflex sensitivity decreased with progression of HS and was reversed with resuscitation. The changes in the BRS that we observed are similar to those reported by Iwasaki et al. (42) in humans subjected to head-down tilt, in which a decrease in BRS paralleled the decrease in RRI HFP. Loss of HRV complexity in our study was associated with a decrease in vagal input to the heart, likely a normal, compensatory response to hypovolemia. However, we cannot exclude the possibility that loss of complexity at lower blood pressures may also represent ischemia-induced uncoupling of cardiovascular and autonomic regulation (43) and impairment of efferent neuronal input to the heart and lungs (32, 44, 45). Because brain injury has also been characterized by decomplexification and low HF and LF powers (7), more data are needed to enable discrimination of brain-injured and HS patients. More data would also be needed to determine the sensitivity and specificity of these new diagnostic measures.

We also found increases in SAP HFP during HS. Julien et al. (46) suggested that respiratory-frequency oscillations (HFP) in arterial pressure involve fluctuations in beat-to-beat stroke volume of mechanical origin. ABP oscillations were found to be mainly caused by the mechanical effect of respiration on intrathoracic pressure. As shown by Saul et al. (47) and deBoer et al. (48), the effect of intrathoracic pressure on stroke volume, in turn, is enhanced by hypovolemia. Autonomic regulation of the HR may also cause vagally mediated changes in the SAP HFP (47).

As shown by Brown et al. (29), breathing frequency and depth are known to

influence HRV profoundly and should be controlled in HRV studies. Because our animals were breathing at a set rate and depth, the influence of lung inflation on RRI responses was constant throughout the experiment. Thus, we can attribute the changes in complexity in this experiment to autonomic rather than mechanical sources (30). Changes in heart rate complexity might be different in patients who are not mechanically ventilated.

A limiting factor affecting HRV metrics is the nonstationarity of the signal. For a stationary time series, the average value of the mean and the SD do not vary with time (15). Signals that do not obey this condition are considered nonstationary.

Nonstationarity affects frequency-domain variables more than it does nonlinear variables. The latter are not immune to the effects of signal nonstationarity (especially fractal scaling). However, some of them—especially the entropy-based measures—quantify statistical order, as they were designed for quantification of regularity in both deterministic and stochastic models (15). New methods not explored in the present study, such as detrended fluctuation analysis that quantifies changes in short- and long-scale components of data sets (49), may be more advantageous for analysis of nonstationary signals.

In an effort to minimize the influence of nonstationarity on the data sets analyzed in this study, instead of continuous data sampling during protocol interventions we chose to analyze waveforms retrieved from periods of time between interventions during which the data were as stable as possible. However, the potential effect of signal nonstationarity on our results cannot be discounted, and our data should be interpreted with caution.

The presence of ectopic beats may alter the results of HRV analysis. Our highest rates of interpolation were 1.5% and 1.8% (in two data sets of 120 analyzed); thus, we believe that the minimal editing of the ectopic beats performed in our study did not significantly affect our results.

Currently, techniques are sought that enable early identification of subjects with "survivable" or "nonsurvivable" injuries, enabling distant decision support and increased situational awareness in mass-casualty or battlefield settings, a concept known as *remote triage*. Assessment of HRV with nonlinear statistical methods may be one such technique. By providing insight into the underlying control mechanisms at work during hemorrhagic shock, it is possible that HRV analysis may augment the information obtained from traditional vital signs such as the pulse and blood pressure. However, studies in human trauma patients are needed and are ongoing. Continuous data analysis with sliding time windows for both spectral and nonlinear analysis (not employed in our study) may help clarify whether and at what point HRV variables may be superior to traditional vital signs.

CONCLUSIONS

This study in anesthetized swine supports the concept that RRI complexity is decreased by hemorrhagic shock. Several complementary measures of complexity were noted to change with shock, to include ApEn, SampEn, and SymDyn. Changes in FDCL were similar but not significant. These alterations in the complexity of the RRI may be mediated by vagal withdrawal, as evidenced by concomitant decreases in RRI HFP and in integrated baroreflex sensitivity. These techniques are now being applied to the analysis of heart rate variability in trauma and burn patients.

REFERENCES

1. Brovelli M, Baselli G, Cerutti S, et al: Computerized analysis for an experimental validation of neurophysiological models of hear rate control. *Comput Cardiol* 1983; 205–208
2. Pagani M, Lombardi F, Guzzetti S, et al: Power spectral analysis of heart rate and arterial pressure variabilities as a marker of sympatho-vagal interaction in man and conscious dog. *Circ Res* 1986; 59:178–193
3. Butler GC, Yamamoto Y, Hughson RL: Fractal nature of short-term systolic BP and HR variability during lower body negative pressure. *Am J Physiol* 1994; 267:R26–R33
4. Goldstein B, Mickelsen D, Want A, et al: Effect of N(G)-nitro-L-arginine methyl ester on autonomic modulation of heart rate variability during hypovolemic shock. *Crit Care Med* 1999; 27:2239–2245
5. Toweill DL, Kovarik WD, Carr R, et al: Linear and nonlinear analysis of heart rate variability during propofol anesthesia for short-duration procedures in children. *Pediatr Crit Care Med* 2003; 4:308–314
6. Cooke WH, Salinas J, Convertino VA, et al: Heart rate variability and its association with mortality in prehospital trauma patients. *J Trauma* 2006; 60:363–370
7. Goldstein B, Fiser DH, Kelly MM, et al: Decomplexification in critical illness and injury: relationship between heart rate variability, severity of illness, and outcome. *Crit Care Med* 1998; 26:352–357
8. Winchell RJ, Hoyt DB: Spectral analysis of heart rate variability in the ICU: a measure of autonomic function. *J Surg Res* 1996; 63: 11–16
9. Eckberg DL: Sympathovagal balance: A critical appraisal. *Circulation* 1997; 96: 3224–3232
10. Pagani M, Malliani A: Interpreting oscillations of muscle sympathetic nerve activity and heart rate variability. *J Hypertens* 2000; 18:1709–1719
11. Kuusela TA, Jartti TT, Tahvanainen KU, et al: Nonlinear methods of biosignal analysis in assessing terbutaline-induced heart rate and blood pressure changes. *Am J Physiol Heart Circ Physiol* 2002; 282:H773–H783
12. Goldberger AL, West BJ: Fractals in physiology and medicine. *Yale J Biol Med* 1987; 60:421–435
13. Buchman TG: Physiologic stability and physiologic state. *J Trauma* 1996; 41:599–605
14. Goldberger AL: Non-linear dynamics for clinicians: chaos theory, fractals, and complexity at the bedside. *Lancet* 1996; 347: 1312–1314
15. Pincus SM, Cummins TR, Haddad GG: Heart rate control in normal and aborted-SIDS infants. *Am J Physiol* 1993; 264:R638–R646
16. Goldberger AL, West BJ: Applications of nonlinear dynamics to clinical cardiology. *Ann N Y Acad Sci* 1987; 504:195–213
17. Makikallio TH, Ristimae T, Airaksinen KE, et al: Heart rate dynamics in patients with stable angina pectoris and utility of fractal and complexity measures. *Am J Cardiol* 1998; 81:27–31
18. Tapanainen JM, Thomsen PE, Kober L, et al: Fractal analysis of heart rate variability and mortality after an acute myocardial infarction. *Am J Cardiol* 2002; 90:347–352
19. Lipsitz LA, Goldberger AL: Loss of "complexity" and aging. Potential applications of fractals and chaos theory to senescence. *JAMA* 1992; 267:1806–1809
20. Kaplan DT, Furman MI, Pincus SM, et al: Aging and the complexity of cardiovascular dynamics. *Biophys J* 1991; 59:945–949
21. Pikkujamsa SM, Makikallio TH, Sourander LB, et al: Cardiac interbeat interval dynamics from childhood to senescence: comparison of conventional and new measures based on fractals and chaos theory. *Circulation* 1999; 100:393–399
22. Ribeiro AL, Lombardi F, Sousa MR, et al: Power-law behavior of heart rate variability in Chagas' disease. *Am J Cardiol* 2002; 89: 414–418
23. Makikallio TH, Hoiber S, Kober L, et al: Fractal analysis of heart rate dynamics as a predictor of mortality in patients with depressed left ventricular function after acute myocardial infarction. TRACE Investigators. TRAndolapril Cardiac Evaluation. *Am J Cardiol* 1999; 83:836–839
24. Makikallio AM, Makikallio TH, Korpelainen JT, et al: Heart rate dynamics predict post-

stroke mortality. *Neurology* 2004; 62: 1822–1826
25. Laitio TT, Makikallio TH, Huikuri HV, et al: Relation of heart rate dynamics to the occurrence of myocardial ischemia after coronary artery bypass grafting. *Am J Cardiol* 2002; 89:1176–1181
26. Goldberger AL, Mietus JE, Rigney DR, et al: Effects of head-down bed rest on complex heart rate variability: response to LBNP testing. *J Appl Physiol* 1994; 77:2863–2869
27. Yamanaka N, Aoyama T, Ikeda N, et al: Characteristics of heart rate variability entropy and blood pressure during hemodialysis in patients with end-stage renal disease. *Hemodial Int* 2005; 9:303–308
28. Palazzolo JA, Estafanous FG, Murray PA: Entropy measures of heart rate variation in conscious dogs. *Am J Physiol* 1998; 274: H1099–1105
29. Brown TE, Beightol LA, Koh J, et al: Important influence of respiration on human R-R interval power spectra is largely ignored. *J Appl Physiol* 1993; 75:2310–2317
30. Badra LJ, Cooke WH, Hoag JB, et al: Respiratory modulation of human autonomic rhythms. *Am J Physiol Heart Circ Physiol* 2001; 280:H2674–H2688
31. Pincus S: Approximate entropy (ApEn) as a complexity measure. *Chaos* 1995; 5:110–117
32. Hornero R, Aboy M, Abasolo D, et al: Complex analysis of intracranial hypertension using approximate entropy. *Crit Care Med* 2006; 34:87–95
33. Richman JS, Moorman JR: Physiological time-series analysis using approximate entropy and sample entropy. *Am J Physiol Heart Circ Physiol* 2000; 278:H2039–H2049
34. Penttila J, Helminen A, Jartti T, et al: Effect of cardiac vagal outflow on complexity and fractal correlation properties of heart rate dynamics. *Auton Autacoid Pharmacol* 2003; 23:173–179
35. West BJ, Scafetta N, Cooke WH, et al: Influence of progressive central hypovolemia on Holder exponent distributions of cardiac interbeat intervals. *Ann Biomed Eng* 2004; 32: 1077–1087
36. Jartti TT, Kuusela TA, Kaila TJ, et al: The dose-response effects of terbutaline on the variability, approximate entropy and fractal dimension of heart rate and blood pressure. *Br J Clin Pharmacol* 1998; 45:277–285
37. Goldstein B, DeKing D, DeLong DJ, et al: Autonomic cardiovascular state after severe brain injury and brain death in children. *Crit Care Med* 1993; 21:228–233
38. Kawase M, Komatsu T, Nishiwaki K, et al: Heart rate variability during massive hemorrhage and progressive hemorrhagic shock in dogs. *Can J Anaesth* 2000; 47:807–814
39. Triedman JK, Cohen RJ, Saul JP: Mild hypovolemic stress alters autonomic modulation of heart rate. *Hypertension* 1993; 21: 236–247
40. Kato M, Komatsu T, Kimura T, et al: Spectral analysis of heart rate variability during isoflurane anesthesia. *Anesthesiology* 1992; 77:669–674
41. Komatsu T, Singh PK, Kimura T, et al: Differential effects of ketamine and midazolam on heart rate variability. *Can J Anaesth* 1995; 42:1003–1009
42. Iwasaki KI, Zhang R, Zuckerman JH, et al: Effect of head-down-tilt bed rest and hypovolemia on dynamic regulation of heart rate and blood pressure. *Am J Physiol Regul Integr Comp Physiol* 2000; 279:R2189–R2199
43. Godin PJ, Buchman TG: Uncoupling of biological oscillators: a complementary hypothesis concerning the pathogenesis of multiple organ dysfunction syndrome. *Crit Care Med* 1996; 24:1107–1116
44. Langhorst P, Schulz B, Schulz G, et al: Reticular formation of the lower brainstem. A common system for cardiorespiratory and somatomotor functions: discharge patterns of neighboring neurons influenced by cardiovascular and respiratory afferents. *J Auton Nerv Syst* 1983; 9:411–432
45. Schulz B, Lambertz M, Schulz G, et al: Reticular formation of the lower brainstem. A common system for cardiorespiratory and somatomotor functions: discharge patterns of neighboring neurons influenced by somatosensory afferents. *J Auton Nerv Syst* 1983; 9:433–449
46. Julien C, Zhang ZQ, Cerutti C, et al: Hemodynamic analysis of arterial pressure oscillations in conscious rats. *J Auton Nerv Syst* 1995; 50:239–252
47. Saul JP, Berger RD, Albrecht P, et al: Transfer function analysis of the circulation: unique insights into cardiovascular regulation. *Am J Physiol* 1991; 261:H1231–1245
48. deBoer RW, Karemaker JM, Strackee J: Hemodynamic fluctuations and baroreflex sensitivity in humans: a beat-to-beat model. *Am J Physiol* 1987; 253:H680–H689
49. Peng CK, Havlin S, Stanley HE, et al: Quantification of scaling exponents and crossover phenomena in nonstationary heartbeat time series. *Chaos* 1995; 5:82–87

APPENDIX

Baroreflex Sensitivity Calculation

Baroreflex sensitivity is calculated automatically by identification of a monotonically increasing or decreasing set of three or more consecutive corresponding data points on the RRI and SAP time series. From the set of SAP and RRI values, an xy-scatter plot is created and a regression line is fitted over the data points. The slope of this line is the BRS.

Nonlinear Variables (11)

Approximate Entropy. ApEn is a measure of the complexity of a signal; it is low in regular signals and high in irregular signals. ApEn determines the conditional probability of finding specific patterns in the time series, i.e., the logarithmic likelihood that a run of patterns that is close remains close on the next incremental comparison. The template patterns are constructed from the signal itself, and no *a priori* knowledge of the system is needed.

Sample Entropy. This is a similar concept to ApEn, with the computational difference that the vector comparison with itself is removed. ApEn occasionally falsely indicates that signals are more regular than they actually are. SampEn corrects for this problem.

Symbol Dynamics Entropy (SymDyn). Four "symbols" are generated (A, B, C, D) by using the mean and SD of the signal to create value "bands" for each symbol: e.g., "A" if signal value $\leq$ (mean $-$ SD), etc. The time series is then converted to a symbol sequence. This symbol sequence is then interpreted as a sequence of three-letter "words." The complexity (Shannon entropy) of the distribution of words is then determined.

Bits per Word. Bit per word is a method of normalizing SymDyn.

Lempel-Ziv Entropy. The signal is converted to a binary sequence (series of 0s and 1s), in which 1 represents values above the mean and 0 represents values below the mean. This kind of sequence can be constructed by two operations: the insertion of symbol(s) to form a subqueue (i.e., a shorter sequence of 0s and 1s) and the copying, or repetition, of this subqueue. For Lempel-Ziv entropy, the complexity of this sequence is determined by the number of such insertion and copying operations that need to be performed to generate the sequence.

Fractal Dimension by Dispersion Analysis (FDDA). FDDA determines the fractal dimension of a time series. A new time series is created, based on the mean of each set of two adjacent values. This process is continued with data sets of four points, 16 points, etc. Log SD(m) is plotted against log m. FDDA is defined as 1-slope. The variable m is the number of data points used to group adjacent data points: 4, 16, etc. FDDA has a value of 1.0–1.5. FDDA = 1 indicates a constant signal, and 1.5 indicates a maximally fractal structure, i.e., a totally random signal.

Fractal Dimension by Curve Lengths. Another method of determining the fractal dimension of a time series. A given curve is conceptualized as consisting of a number of short segments. FDCL counts the number of such segments of various lengths needed to follow the curve.